ROYAL SOCIETY
OF CHEMISTRY

Check for updates

Bio-degradable, fully bio-based, thermally cross-linked superabsorbent polymers from citric acid and glycerol†

Jingying Chen,[a] Deelan Yen Chan,[b] TaoTao Yang,[a] Daniele Parisi, [ID] [a] Bart Reuvers,[b] Theo Veldhuis,[b] Francesco Picchioni, [ID] [a] Jing Wu, [ID] *[c] Patrizio Raffa [ID] *[a] and Cor Koning[a,b]

In this study, cross-linker free, fully bio-based, biodegradable superabsorbent polymers (SAPs) were synthesized from the multi-functional monomers citric acid (CA), monosodium citrate (MSC) and glycerol (GLY) by polycondensation and subsequent thermal self-cross-linking. All monomers (CA, MSC, GLY) used in this study were not only bio-based but also non-toxic. All of them contain more than two hydrophilic groups in one molecule, which shows great potential to be used in the production of SAPs. The structure, water absorbance capacity and biodegradability of the resulting SAPs were investigated in detail. Upon removal of the soluble fraction, the SAPs have a gel content of approximately 60% and exhibit a maximum absorption capacity of deionized water of 24 ± 2 g g^{-1}. Moreover, the prepared SAPs show good biodegradability at 25 °C (40% biodegradability after 28 days) in an activated sludge-containing medium and are accordingly promising eco-friendly materials for potential use in our environment, not generating persistent microplastics like commercial non-biodegradable SAPs based on neutralized polyacrylic acid and polyacrylamides. Therefore, the bio-based SAPs described in this paper have promising application potential for the sustainable chemical industries including hygiene products and agricultural products, *e.g.* controlled-release fertilizer coatings and soil improvers.

Green foundation

1. Superabsorbent polymers, largely used in the personal care and agricultural industries, are one major source of microplastics and carbon emissions, as they are typically fossil-based, non-recyclable and non-degradable. We propose here a new fully bio-based and bio-degradable formulation for such materials, making them more environmentally friendly.

2. Our superabsorbent polymers are made only of renewable building blocks and show a water absorption capacity of 2400% and a biodegradability of 40% in 28 days.

3. Water absorbency and biodegradability could be further improved by trying different formulations. For example, different bio-based molecules with multiple hydroxyl and carboxylic functionalities can be tested, and/or different counterions.

1. Introduction

Superabsorbent polymers (SAPs) are a class of cross-linked hydrophilic polymers that can absorb substantial amounts (usually more than 10 g g^{-1}) of water and retain it even under pressure.[1] Taking the most successfully commercialized SAP class, *viz.* polyacrylates, as an example,[2] these can absorb more than 100 times their own weight of distilled water. Because of their unique absorbing ability, they have been widely used in different fields, including hygiene products, agriculture, construction and so forth, of which hygiene products (such as baby diapers, female sanitary, and adult incontinence pro-

[a] Smart and Sustainable Polymeric Products, Department of Product Technology, Engineering and Technology Institute Groningen, University of Groningen, Nijenborgh 3, 9747 AG Groningen, The Netherlands. E-mail: p.raffa@rug.nl
[b] Covestro (Netherlands) B.V., Ceintuurbaan 5, 8022 AW Zwolle, The Netherlands
[c] Co-Innovation Center for Textile Industry, Innovation Center for Textile Science and Technology, Donghua University, Shanghai 201620, PR China
†Electronic supplementary information (ESI) available. See DOI: https://doi.org/10.1039/d4gc06323f

ducts) take more than 95% market share.[3] Given the increasing birth rate and the average human lifespan around the world, the market of SAPs is projected to grow from 9.0 billion USD in 2019 to 12.9 billion USD by 2024 at a Compound Annual Growth Rate (CAGR) of 7.4% with a global production capacity of over 4 126 000 tons per year in 2020.[2,4]

As mentioned above, the most successfully commercialized SAPs are polyacrylates, including neutralized polyacrylic acid and polyacrylamide. They have unmatched water absorbance capacities, which are related to the highest possible hydrophilic group density (one hydrophilic group in each repeating unit consisting of merely two carbon atoms in the backbone). However, the backbone fully consisting of carbon–carbon bonds endows polyacrylates with a stable structure even under harsh conditions and thus implies poor or even zero biodegradability. Furthermore, for hygiene applications, it is difficult to reuse these severely contaminated materials, which means that most likely the SAPs in these products will turn out to be a source for microplastics after use. In the near future, legislation banning the use of non-biodegradable and persistent microplastics will come into force.[5] In view of the clear global trend of banning the use of disposable plastic products in the (near) future, especially persistent microplastic-generating species, it is necessary to develop biodegradable alternatives to tackle the microplastic issue.

To date, most researchers focus on natural polymer-based SAPs such as cellulose,[6,7] chitosan,[8–10] starch,[11–13] proteins,[14,15] etc. In these studies, bio-based SAPs are produced by graft-copolymerization of acrylic acid or derivatives onto those natural polymers described above. It has been reported that these SAPs show great absorbance capacity and also biodegradability to some extent. However, there are still two shortcomings: firstly, these natural polymers usually have ultra-high molecular weight, which makes it difficult to handle them during the production of SAPs;[16] secondly, the biodegradability of these resulting SAPs mostly arises from the natural polymer moieties, while the (poly)acrylic acid moieties are non-biodegradable.[17,18] Given the high content of acrylic acid in these SAPs, the remainder of these products, after being subjected to biodegradation, is still harmful to and persistent in the environment and can still end up in our food chain.

In 2017, a Korean research group[16] introduced a promising step-growth method with high potential to produce polycondensate-type citric acid (CA)-based SAPs by melt polymerization. The maximum absorbency of the SAPs produced by this method was around 22 g g^{-1} of distilled water, which was not as high as the absorbency of acrylic acid-based SAPs, but nevertheless this product blazed a new trail to synthesize novel synthetic and potentially biodegradable SAPs. The authors reported bio-based SAPs synthesized from citric acid, monosodium citrate and 1,4-butanediol, cross-linked by hexamethylene diisocyanate (HDI). The water-absorbing capacity was studied in detail in that work. However, a biodegradability study of these SAPs, crucial in view of the upcoming legislation on microplastics, was not performed.

In order to avoid the use of toxic cross-linkers like HDI and investigate the potential biodegradability of the CA-based SAPs, in the current study, citric acid and glycerol are chosen as starting monomers to produce fully bio-based SAPs. Compared with 1,4-butanediol, glycerol bears one more hydroxyl group per molecule, which can further react with CA. This makes it possible to avoid the use of additional cross-linkers and still obtain a stable 3D network required for the structural integrity of the SAP and to have good performance. The proposed formulation makes it possible, since both monomers are trifunctional and should therefore be able to self-cross-link, of course depending on the temperature applied.[19] Sufficient neutralization is important for generating SAPs which can deliver enough osmotic pressure difference with the environment. In this study, part of the CA will be replaced by monosodium citrate (MSC) for both introducing neutralization and limiting cross-linking. Here, the neutralization degree (ND) is a number indicating the degree of neutralization of the –COOH groups of citric acid residues in the polymer by sodium hydroxide. CA/GLY-based SAPs with different NDs were synthesized by polycondensation and thermal cross-linking at elevated temperatures and the biodegradability of the resulting SAPs was characterized in detail.

2. Materials and methods

2.1. Materials

Citric acid (CA, ≥99.5%), glycerol (GLY, ≥99.5%), monosodium citrate (MSC, 99%), ethylene glycol (EG, 99.8%), monobasic potassium phosphate (≥99.0%), dibasic potassium phosphate (≥98.0%), disodium hydrogen phosphate dehydrate (≥99.0%), ammonium chloride (≥99.5%), calcium chloride (≥93.0%), magnesium sulfate heptahydrate (≥98%), iron(III) chloride hexahydrate (97%), and sodium acetate (≥99%) were purchased from Sigma-Aldrich and used without further purification. Deionized water was purified with WaterPro PS Polishing Systems equipment purchased from the LABCONCO Company. The water containing activated sludge was taken from a water treatment center in Glimmen (Province of Groningen, The Netherlands). E-D-SCHNELLSIEB PAINT STRAINER super fine 125my (blue mesh) filter paper was kindly supplied by Covestro (The Netherlands) B.V. Regenerated cellulose filter paper (pore size: 0.45 μm) for insoluble content determination was purchased from SARTORIUS Biotech GmbH (Germany).

SAP precursor polymer synthesis. SAPs of various compositions were synthesized from CA, GLY and MSC via a bulk two-step polycondensation procedure using equimolar feed ratios of (CA + MSC)/GLY in all cases (see Table 1): a 500 mL, three-neck flange flask equipped with a mechanical stirrer, a Schlenk line, and a condenser were purged with a nitrogen–vacuum cycle three times at room temperature to remove air. In the beginning, CA, GLY and MSC in the desired molar ratios were put in the flange flask, and a small amount of deionized water was added to help the dissolution of CA into

Table 1 Molecular weight and insoluble content of the as-synthesized CA/GLY-based SAP precursor polymers before the thermal cross-linking treatment

SAP precursor polymer	SAP	CA : MSC : GLY molar feed ratio	M_n^a (×10³ g mol⁻¹)	M_w^a (×10³ g mol⁻¹)	PDI	Insoluble content[b] (%)
PGC	SAP-0	10 : 0 : 10	0.7	17.9	31.4	62
PGC$_{90}$M$_{10}$	SAP-10	9 : 1 : 10	0.7	15.4	21.3	43
PGC$_{80}$M$_{20}$	SAP-20	8 : 2 : 10	0.7	6.3	9.5	23
PGC$_{70}$M$_{30}$	SAP-30	7 : 3 : 10	0.7	5.6	9.0	0
PGC$_{60}$M$_{40}$	SAP-40	6 : 4 : 10	0.7	5.6	8.8	0
PGC$_{50}$M$_{50}$	SAP-50	5 : 5 : 10	0.6	4.0	6.8	0
PGC$_{40}$M$_{60}$	SAP-60	4 : 6 : 10	0.7	3.2	4.4	0
PGC$_{30}$M$_{70}$	SAP-70	3 : 7 : 10	0.5	1.1	2.8	0
PGC$_{20}$M$_{80}$	SAP-80	2 : 8 : 10	0.6	4.3	6.2	0
PGC$_{15}$M$_{85}$	SAP-85	1.5 : 8.5 : 10	0.6	5.6	9.0	0
PGC$_{10}$M$_{90}$	NA[c]	1 : 9 : 10	0.6	5.6	9.0	0
PGM		0 : 10 : 10	0.7	6.0	9.0	0

[a] Based on PEG standards; values for soluble fractions only. [b] This is calculated according to eqn (1); the pore size of the filter paper is 0.45 μm. [c] Not applicable because the material is water soluble, thus it cannot be regarded as a SAP.

GLY to obtain a homogeneous solution. Polyesterification was performed in two steps: firstly, it was done at 130 °C under a mild nitrogen flow for 3 h. After that, the reaction was finished in the same flask at 130 °C under vacuum (about 1 mbar) with the condenser replaced by a glass plug and the water would be collected by a cold trap surrounded with liquid nitrogen. After reaction for 4.5–6 h in total, the mechanical stirrer was stopped because of the high viscosity of the SAP precursor polymer. In the meantime, an obvious Weissenberg effect could be observed on the stirring blade in the flask, which illustrated the relatively high molecular weight of the SAP precursor polymer. After the reaction, the product was cooled down to room temperature and taken out of the flask. After pulverizing and drying, the molecular weight of the fully soluble product was characterized by GPC analysis in water (details can be found below) and the material was stored at room temperature before thermal cross-linking was performed.

Thermal cross-linking and washing. The SAP precursor polymers synthesized as described above, before being subjected to a cross-linking treatment, were pulverized by an IKA Tube Mill control for 3 min at room temperature to yield fine powders (with a particle size of around 50–100 μm, as characterized by a digital microscope, Keyence VHX-7000 series). The fine powders were then evenly spread in a hand-made, open cuboid aluminium box and put into an oven at 140 °C under a vacuum of about 0.1 mbar for 1 h to induce thermal cross-linking. After the thermal cross-linking treatment, the powders turned out to be transformed into fluffy materials. This obtained material was extracted with water to separate the soluble fraction. The gel content, in fact the SAP yield after the cross-linking step, is an important parameter for the production of SAPs. This insoluble part of the SAP was determined and calculated in this work as follows: M_1 g ground (details can be found in the Thermal cross-linking section) SAPs were immersed in an excess of de-ionized water and stirred for 1 h to ensure sufficient swelling. After that the mixture of swelled SAPs and the test

medium were filtered via the super fine 125my (blue mesh) filter paper (original weight filter paper: M_2 g) mentioned in the Materials section in this paper. Then the filter paper and swelled SAP particles were dried at 60 °C under vacuum in the oven for 24 h. After that, the filter paper and SAPs were weighed together as M_3 g.

$$\text{Gel content (\%)} = (M_3 - M_2)/M_1 \times 100\%. \quad (1)$$

In the context of the following discussion, the SAPs obtained before washing are indicated as 'unextracted SAPs' and after washing as 'extracted SAPs'. After extraction, the materials were ground again using an IKA Tube Mill control to deliver fine powders (with a particle size of around 50–100 μm, as characterized by a digital microscope, Keyence VHX-7000 series; grinding times are mentioned in the Results and discussion section), which were stored in a desiccator at room temperature before further characterization.

2.2. General methods

Insoluble content determination of SAP precursor polymers. It should be noted that even before the thermal cross-linking treatment, the SAP precursor polymers may already contain some insoluble gel parts, formed during the polycondensation reaction. The insoluble content of the SAP precursor polymer in water was determined by a Buchner vacuum filtration funnel connected to a Kitasato flask, equipped with a KNF Laboport vacuum pump. 3 g of SAP precursor polymer was weighed and added to 20 ml of deionized water and subsequently stirred for 30 min. The solution/dispersion (including the insoluble part) was filtered using the SARTORIUS regenerated cellulose filter paper (pore size: 0.45 μm, Sartorius Biotech GmbH, Germany) on the Buchner funnel. The insoluble content was calculated using the equation below:

$$\text{Insoluble content} = m_0/m_1 \times 100\% \quad (2)$$

where m_1 is the original weight of the SAP precursor polymer to be analyzed and m_0 is the weight of the insoluble part of this SAP precursor polymer.

Subsequently, the soluble part of the SAP precursor polymer was further filtered with Corning® syringe filters (a regenerated cellulose membrane, diam. 15 mm, pore size 0.2 μm) and used for the GPC analysis.

GPC analysis. Gel permeation chromatography (GPC) in water was performed on the SAP precursor polymers with an Agilent Technologies 1200 series, equipped with three 300 × 8 mm PPS Suprema columns (100, 1000, 3000 Å; column temperature 40 °C) in series with a RID detector. The samples were prepared by dissolving the SAP precursor polymer mentioned above in deionized water at a concentration of 10 mg mL^{-1} and using ethylene glycol as the internal standard. The samples were eluted with 0.05 M NaNO$_3$ at a flow rate of 1 mL min^{-1}. Molecular weights and polydispersity indexes (PDIs) were determined using the software PSS WinGPC unity from Polymer Standard Service. Polyethylene glycol standards (M_p = 194, 610, 1470, 3860, 16 100, 28 230, 68 900, 117 900, 538 000 and 1 039 000 Da) were used for calibration.

FTIR analysis. Fourier Transform Infrared (FTIR) spectra were recorded using a Shimadzu IR-Tracer-100 with a golden gate diamond attenuated total reflectance (ATR) sample unit in the range of 4000 cm^{-1} to 500 cm^{-1} at a resolution of 4 cm^{-1} and averaged over 32 scans.

Elemental analysis. Elemental analysis of all SAPs, including unextracted SAPs, extracted SAPs and the soluble parts, was carried out using an automated Euro Vector EA3000 analyzer with acetanilide as a calibration reference. The content of C, H and Na was determined assuming that no other elements are present, and the oxygen content was estimated by difference. All the samples were analyzed three times, and the average values are reported in this study.

In addition, the content of C, O and Na could also be determined by energy dispersive spectroscopy (EDS). The elemental composition (*viz.* C, O and Na) was determined using a JSM-6320 scanning electron microscope operating at an accelerating voltage of 15 kV and the results were analyzed using EDAX TEAM software. The weight fractions of C, O and Na can be obtained directly from the EDS spectrum, while the proton (H) content was estimated from the difference to 100% of the values obtained for C, O and Na. All samples were analyzed at three different positions, and the average values obtained for each element are reported in this work.

Particle size and specific surface area characterization. The particle size of the extracted SAPs was characterized in two ways in this work:

(a) By scanning electron microscopy (SEM): SEM analysis was carried out on a JSM-6320 instrument with an accelerating voltage of 2 kV, and the samples were sputtered with Pt/Pd prior to SEM observation.

(b) By digital microscopy (DM): DM analysis was carried out on a Keyence digital microscope (VHX-7000 series, produced by the KEYENCE INTERNATIONAL Company, Belgium). A typical procedure is as follows: 20–50 mg samples were spread as evenly as possible at the center of a microscope slide and the areas with mostly single-layered samples were chosen for the measurement. A picture was taken by the computer con-nected to the microscope. The outliers, both over-sized and extremely small, were eliminated according to the area and circularity values, and the rest of the particles were chosen and characterized based on the particle size by the computer automatically. All the parameters described below are defined as follows: D_{min} is the minimum possible distance between two parallel lines on either side of the particle. D_{max} is the maximum length between any two points that lie on the inner perimeter of the figure. The perimeter is the length of the perimeter of the figure. When the figure is a perfect circle, the circularity index is 1; when it becomes long and thin, the value approaches 0. $D_{circle\ equivalent}$ is the diameter of a circle with the same area as the figure. More details can be found in the ESI.†

The specific surface area of the extracted SAPs was calculated after performing a Brunauer–Emmett–Teller (BET) analysis. Nitrogen adsorption–desorption isotherms were measured at −196.15 °C on a Micromeritics Tristar 3000 after a pretreatment at 40 °C for 5 h under a N$_2$ atmosphere to remove residual water.

Rheological analysis. The cross-link density of different SAPs was determined indirectly by rheological measurements. The measurements have been performed with a Physica MCR302 rheometer equipped with an 8 mm diameter plate/plate geometry. The temperature was controlled by a Peltier hood and a Peltier bottom plate. The 100% solid, extracted porous SAP powder was positioned on the bottom plate at a temperature sufficiently high to make the vitrified cross-linked powder compressible and sufficiently low to avoid any chemical reactions. Subsequently, the upper plate was lowered to compress the porous rubbery powder into a massive sample. The amount of powder positioned between the plates was adjusted to result in a compressed sample height within the range of 400–700 μm. After completion of the compression, the actual rheological measurement was started. *Via* the upper plate, the sample was subjected to an oscillatory shear deformation $\gamma(t)$ with an amplitude (γ_0) of 0.05% and a frequency of 1 Hz. The amplitude of the resulting oscillatory shear stress $\tau(t)$ is referred to as τ_0. The phase shift between the oscillating stress and oscillating deformation is referred to as δ. From the measured values of τ_0, γ_0 and δ, the storage modulus G' and the loss modulus G'' were derived. These rheological characteristics have been acquired as a function of temperature, while cooling the sample at a rate of −1 °C min^{-1}.

Absorption speed test. 2 g cross-linked and extracted SAP powders were put into a 100 mL glass jar and immersed in deionized water (DW) for different times (1, 2, 3, 4, 5, 10, 15, 20, 25 and 30 min) and then the solution was filtered through the filter paper. The calculation is as indicated in the text below.

Total free water absorption test until saturation. 2 g cross-linked and extracted SAP powders were put into a 100 mL glass jar and immersed in deionized water. After stirring for a couple of seconds, the dispersions were allowed to stand for 30 min, after which the solution was filtered through the filter paper until no more water dripping was observed. The residue

was weighed for the calculation given below. The filtrate was collected for subsequent elemental analysis on extracted and unextracted SAPs. The total free water absorption (WA) was calculated as follows:

$$WA = (W_2 - W_1)/W_1 \ (g \ g^{-1}) \tag{3}$$

where W_1 is the original weight of the (dry) SAP and W_2 is the weight of the SAP after swelling. It should be noted that margins of error are based on differences observed for measurements performed in triplicate.

Biodegradability test. The biodegradability test was performed using a Biochemical Oxygen Demand (BOD) determination machine (BD 600 series, produced by Lovibond Company). A predetermined amount of the test substance was added to the test medium (water containing activated sludge). The solution was kept in a closed bottle in the dark at a constant temperature (25 °C), and the biodegradation was followed by measuring the biochemical oxygen demand. The BOD of a substance is an expression for the amount of oxygen consumed by the decomposition of organic matter in a biochemical process. The details about the procedure and method to prepare the samples can be found in the ESI.† In

agreement with the biodegradation test standard for polymers (OECD 301),[20–22] the incubation lasted for 28 days. All the samples were analyzed in duplicate, and the average values are reported in this study.

3. Results and discussion

3.1. Synthesis and characterization of SAP precursor polymers

In this work, SAP precursor polymers (PGC$_x$M$_y$) were synthesized from citric acid (CA), glycerol (GLY), and monosodium citrate (MSC), where x and y represent respectively the molar percentage of CA and MSC in the total amount of acid monomers (CA + MSC) in the feed (Scheme 1). It should be mentioned that in the beginning, to help dissolve CA into GLY, 2 mL of deionized water were added to the flask, resulting in a homogeneous mixture. After 3 hours at 130 °C, all the by-products (including the water added in the beginning and condensation water resulting from the esterification) were collected. At that time point, esterification was regarded as complete, after which no liquid could be collected anymore. Then the reaction was continued in a second step
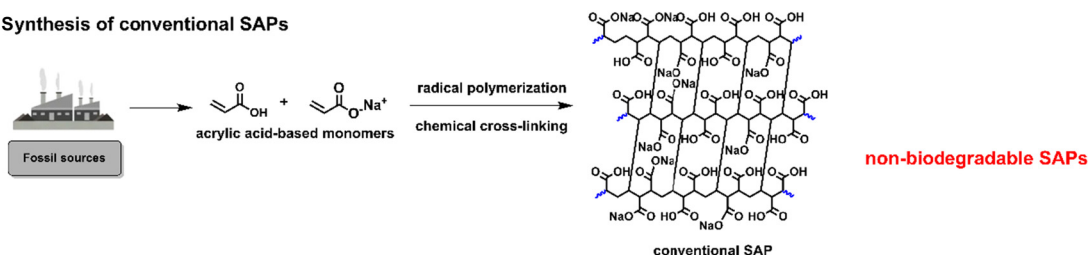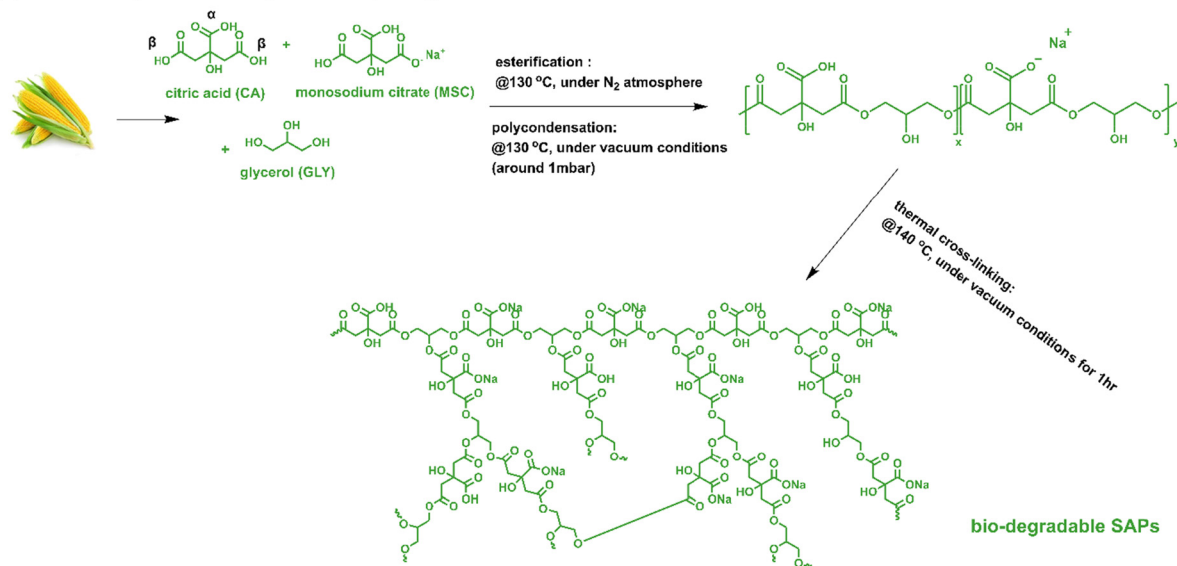
Scheme 1 Comparison between the synthesis of CA + MSC/GLY-based SAPs and conventional SAPs. x denotes the molar percentage of citric acid in the total moles of acid (CA + MSC) in the feed.
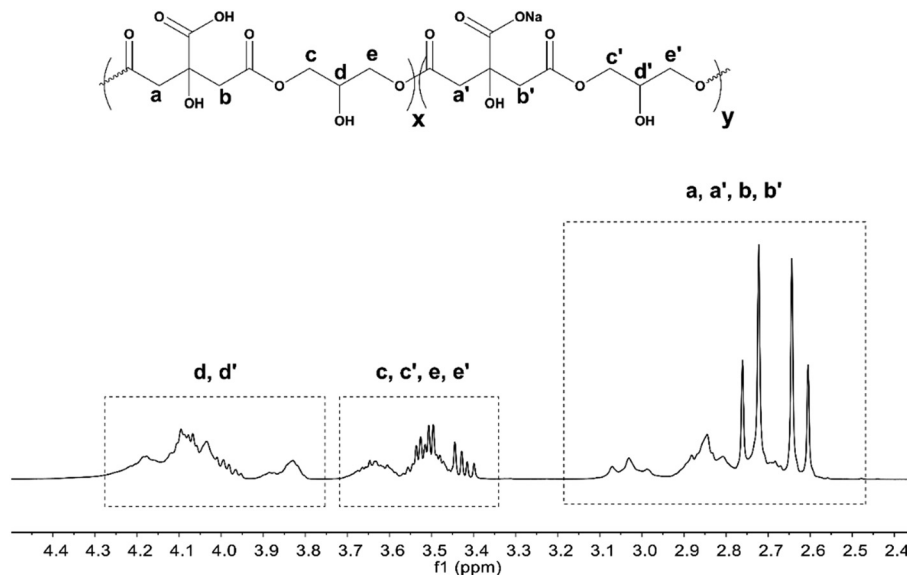
Fig. 1 NMR spectrum of the PGC$_{70}$M$_{30}$ SAP precursor polymer (all peaks were assigned according to the literature reported by Mohammadifar *et al.*[24]).

under vacuum for 1.5–2 hours. Taking PGC$_{70}$M$_{30}$ as an example, a typical ^{1}H spectrum is depicted in Fig. 1. The number and weight average molecular weights and the polydispersity indexes of all synthesized SAP precursor polymers are shown in Table 1. PGC, prepared without the addition of MSC, has the highest M_n (0.7×10^3 g mol^{-1}), M_w (17.9×10^3 g mol^{-1}) and polydispersity index (31.4), which is due to the high average functionality of the monomers (3). This shows the oligomeric nature of these precursors. It has to be noted that in samples with a MSC molar content of up to 20%, insoluble particles were formed, and these were filtered off before performing molecular characterization. Because of the lower reactivity and the lower functionality (2) of MSC,[23] the molecular weight of the resulting SAP precursor polymers made from CA, MSC and GLY decreases with increasing MSC content up to 40 mol%. The GPC data indicate a low functional group conversion and a low degree of polymerization which, as expected, resulted in a predominantly non-cross-linked structure, illustrated by the low values of the insoluble content index, also presented in Table 1. The relatively high polydispersity also suggests branching. This is virtually unavoidable, as there are always trifunctional CA and GLY in the mixtures. Concerning the GLY, some selectivity of primary hydroxyl groups over secondary ones can be expected, limiting branching and cross-linking, as shown in our previous study.[25] It should also be mentioned that the pore size of the filter paper (micrometer grade) used for measuring the insoluble content index is much bigger than the pore size of the membrane filter put in front of the column used for GPC measurements. So, the insoluble content index values are rather approximations than accurate values, and it is possible that cross-linked materials also exist for samples with higher than 20% MSC content. However, this does not affect the following synthetic step.

3.2. Optimization of cross-linking temperature and grinding time for SAPs

Cross-linking and physical properties such as particle size can influence the absorbing performance of SAPs. If not sufficiently cross-linked, the highly hydrophilic polymer chain may be soluble in water, not being capable of trapping any water. On the other hand, too much cross-linking limits the swelling and therefore the absorption capability of the material. To ensure sufficient absorbance capacity, these SAP precursor polymers were thermally cross-linked at elevated temperatures. Compared with chemical cross-linking, thermal cross-linking is more environmentally friendly, avoiding the usage of usually toxic cross-linking agents such as N,N′-methylenebisacrylamide (MBA)[26,27] and hexamethylenediisocyanate.[15] In addition, by controlling and optimizing the thermal cross-linking conditions, SAPs could be generated with as low as possible, but sufficient, cross-link density to build a stable 3D network exhibiting a maximum degree of swelling by water absorption. In this work, it was found that for cross-linking temperatures below 140 °C, the efficiency of the cross-linking process was poor and therefore the temperature range from 140 to 165 °C was studied here. Fig. 2(a) shows the results of the water absorption capacity tests for SAPs with the same overall composition, all having a theoretical neutralization degree (ND) of 80%, but thermally cross-linked at different temperatures.

For a cross-linked polymer, at temperatures $\gg T_g$, all elastic resistance against deformation ($= G'$) originates from the stretching of the cross-linked polymer network chains. At these elevated temperatures, the cross-linked polymer behaves like a rubber. According to the theory of rubber elasticity, at temperatures $\gg T_g$, the plateau modulus, in the absence of entanglements, is solely due to the presence of cross-links
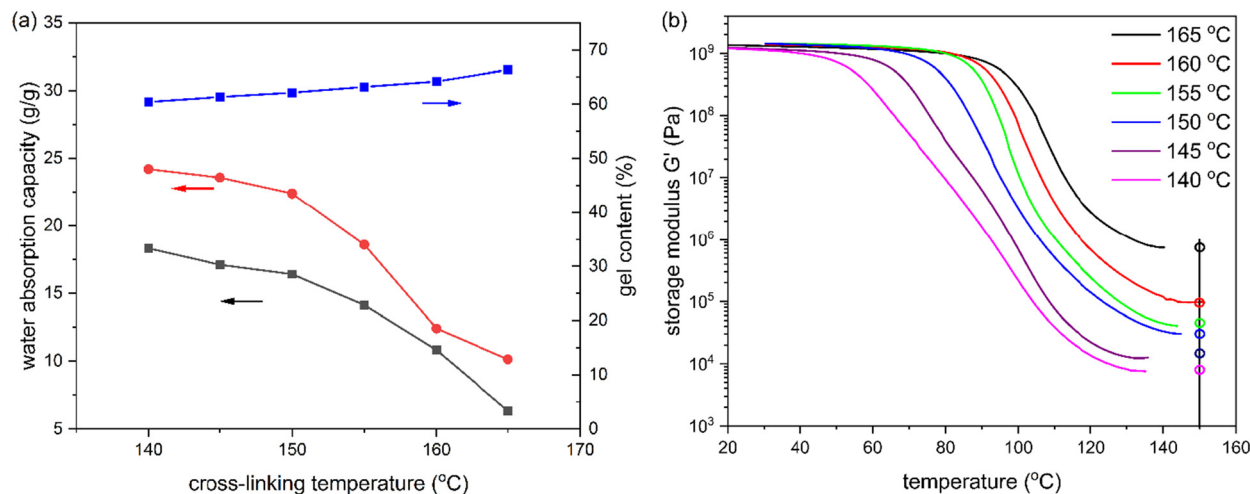
Fig. 2 (a) Water absorption capacity and gel content of SAPs (all variations of SAP-80) *versus* cross-linking temperature; (■) water absorption capacity of unextracted SAP-80s (ground for 180 s), (●) water absorption capacity of extracted SAP-80s (ground for 180 s); (■) gel content of extracted SAP-80s (ground for 180 s); note: all the data shown in the figure are average values based on the results obtained for three separate measurements and the margins of error are ± 2 g g^{-1} for the water absorption capacity test and $\pm 0.2\%$ for the gel content test. (b) Storage modulus as a function of temperature of extracted SAP-80s cross-linked at different temperatures (140 °C to 165 °C) for 1 h *versus* temperature and ground for 180 s. Note: 150 °C (vertical black line) was chosen as the point where G_x was taken; since all curves reached a plateau before 150 °C, it is reasonable to predict the G' value according to the existing curve. The circles are the predicted point at 150 °C.

(G_x), and it is proportional to ν_e, the number of moles of elastically active network chains per m^3 of the examined sample:

$$\nu_e = G_x/RT \tag{4}$$

where G_x is obtained from the rubbery plateau. T is the temperature in K and R is the gas constant (8.314 J K^{-1} mol^{-1}). Using ν_e one can calculate M_c (kg mol^{-1}), the averaged molar weight of the network chains in between two consecutive network junctions:

$$M_c = \rho/\nu_e \tag{5}$$

Here ρ = density (kg m^{-3}). The unit of M_c is kg mol^{-1}.

Upon cross-linking at higher temperatures for the same reaction time (1 h), the obtained SAPs have a higher cross-link density, as proved by the higher plateau storage moduli (G') at elevated temperatures above their T_g (Fig. 2(b)). It should be noted that the different SAPs made in this study are encoded according to the ND. Taking SAP-80 as an example, the SAP cross-linked at 140 °C for 1 h shows the highest water absorption capacity (24 $\pm$ 2 g g^{-1}, extracted SAP; note: the error of ± 2 g g^{-1} is based on the results obtained for three separate measurements). Based on the results shown in Fig. 2(a), 140 °C was chosen as the optimal temperature for the thermal cross-linking process of all SAPs in this study. The water absorption capacity *versus* cross-linking temperature curves of both extracted and unextracted SAPs show the same trend.

It has been reported before that the water absorption rate can also be influenced by the particle size of SAPs.[28] Commonly, the smaller the particle is, the larger the effective surface area the particle has, and thus the faster the water absorption rate the particle is expected to exhibit. However, if the particle size is too small, gel blocking will take place.[29–31] Gel blocking occurs when water initially adsorbed on the surface of SAP particles forms a hydrogel with the cross-linked polymeric material, which inhibits water diffusion to the interior of the SAP particle. In order to avoid gel blocking, the particle size of SAPs should not be too small. It should be mentioned that the experimental way of making the SAP particles makes it difficult to obtain SAPs with varying chemical compositions and NDs with exactly the same particle size, but the grinding time after the thermal cross-linking process can be controlled and the relationship between the grinding time and the resulting particle size can be established. In Fig. 3(a), SEM images of SAP-80 particles are shown for grinding times varying from 30 to 210 s, clearly showing that the SAP particles become smaller and smaller with increasing grinding time. In Table 2, the particle size and circularity index of SAP-80 pulverized for different periods are shown. The calculation method for different indexes can be found in the ESI.† When the grinding time is no more than 30 s, the average values of D_{max} and $D_{circle\ equivalent}$ of the sample are over 200 μm, while the shape of the particles is extremely irregular (the average circularity index is 0). When the grinding time increases, the particles of all samples exhibit a more regular shape (the average circularity index is 1). Like the SEM images shown in a more qualitative way, the more quantitative analysis presented in Table 2 also shows that with increasing grinding time, the particle size decreases, in this case until 240 s. For longer grinding times, the average values of D_{max} and $D_{circle\ equivalent}$ seem to level off. For six different grinding times, varying from 30 to 210 s, for thermally cross-linked (cross-linking temperature: 140 °C) and extracted SAP-80 samples with varying average $D_{circle\ equivalent}$ particle sizes between 250 and 28 μm, the corresponding water
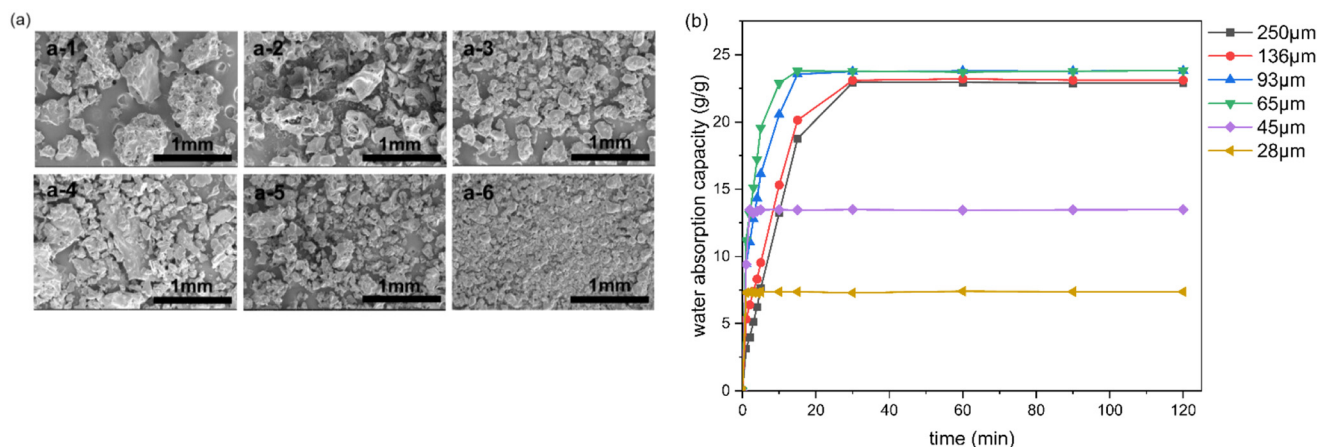
Fig. 3 (a) SEM images of cross-linked (at 140 °C) and extracted SAP-80 particles ground for different times (30, 60, 120, 150, 180, and 210 s, respectively); (b) plot of water absorption capacity *versus* swelling time (samples: cross-linked (at 140 °C) and extracted SAP-80, ground to $D_{\text{circle equivalent}}$ values of 250, 136, 93, 65, 45 and 28 μm obtained after grinding times varying from 30 to 210 s, respectively).

Table 2 Particle size, circularity and BET specific surface area characterization of cross-linked (at 140 °C),ground SAP-80 samples (after extraction) with different grinding times. Particle characteristics determined and analyzed using a Keyence digital microscope (VHX-7000 model) and a Micromeritics Tristar 3000 analyzer

Entry	Grinding time (s)	$D_{\min}{}^a$ (μm)	$D_{\max}{}^b$ (μm)	Perimeter^c (μm)	Area^d (μm^2)	Circularity^e	$D_{\text{circle equivalent}}{}^f$ (μm)	BET specific surface area (m^2 g^{-1})
				Average value				
1	30	234	302	1866	31 053	0	250	0.0555
2	60	123	196	708	15 093	1	136	0.9543
3	90	107	165	666	10 188	1	107	NA^g
4	120	89	139	588	6907	1	93	1.1666
5	150	73	88	350	4854	1	78	NA
6	180	58	72	304	3320	1	65	1.2668
7	210	41	63	248	1821	1	45	1.6731
8	240	23	35	120	607	1	28	2.1167
9	270	25	30	122	594	1	29	NA
10	300	22	30	117	581	1	27	NA

^{a} This is the minimum possible distance between two parallel lines on either side of the particle. ^{b} The maximum length between any two points that lie on the inner perimeter of the figure. ^{c} The length of the perimeter of the figure. ^{d} The area of the graphic. ^{e} When the figure is a perfect circle, the circularity index is 1; when it becomes long and thin, the value approaches 0. ^{f} This is the diameter of a circle with the same area as the figure. ^{g} NA indicates that the BET specific surface area for that sample was not determined.

absorption capacity tests were performed. For these SAP-80 particles, Fig. 3(b) shows the water absorption capacity *versus* swelling time plot. Particles with $D_{\text{circle equivalent}}$ values of 250, 136, 93 and 65 μm, obtained after grinding times of 30, 60, 120, and 180 s, respectively (see Table 2), have comparable maximum absorption capacities (24 ± 2 g g^{-1} in distilled water) after 30 min. However, smaller size particles exhibiting a higher surface area (see Table 2; Brunauer–Emmett–Teller (BET) specific surface areas of 0.0555 m^2 g^{-1} for particles with $D_{\text{circle equivalent}}$ values of 250 μm to 1.2668 m^2 g^{-1} for particles with $D_{\text{circle equivalent}}$ values of 65 μm) can absorb water faster, illustrated by the steeper initial slope going from 250 to 65 μm (Fig. 3(b)). Interestingly, if the SAPs are ground longer, thereby yielding smaller particle sizes (45 and 28 μm), a sharp decreasing trend in the maximum water absorption capacity is observed, which is due to the earlier mentioned gel blocking

effect related to too small particle sizes (please see above). Nevertheless, the water absorption speed of these smaller particles is still high. Based on the observations, in this work, 180 s was chosen as the optimal grinding time for the production of all SAPs with different ND values, resulting in a circle equivalent particle diameter of 65 μm. Based on these results obtained for SAP-80, also for other SAPs with different NDs, this grinding time was applied, which resulted in comparable circle equivalent particle diameters of 56–72 μm.

3.3. Structural characterization of SAPs

Based on the determination of the optimum cross-linking temperature as described above, all SAP precursor polymers were thermally cross-linked at 140 °C for 1 hour (these cross-linking conditions were optimized according to the absorption property test, for which details can be found in Fig. 2), and
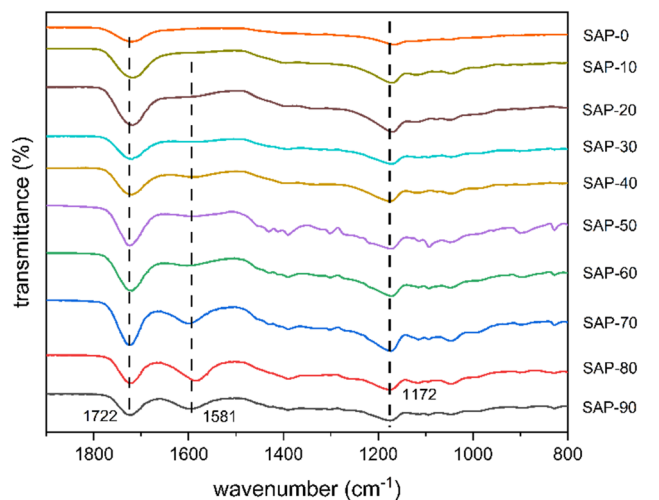
Fig. 4 FTIR spectra of extracted SAPs synthesized from CA, MSC, and GLY and after thermal cross-linking. Molar feed ratio of (CA + MSC)/GLY is always 1/1, weighed in molar monomer ratios CA/MSC (%ND) indicated in the figure.

Fig. 5 Storage modulus of extracted SAP-10 to SAP-80 *versus* temperature. Note: 170 °C (vertical black line) was chosen as the point where G_x was taken; since all curves reached a plateau before 150 °C it is reasonable to predict the G' value according to the existing curve. The circles are the predicted point at 150 °C.

then the resulting network structures (named SAPs) were characterized by FTIR. FTIR spectra for extracted SAPs are shown in Fig. 4. The peaks at 1722, 1581 and 1172 cm^{-1} correspond to the carbonyl C=O of the β-ester carbonyl group, the carboxylate carbonyl group connected to sodium ions and the C–O of the β-ester carbonyl group, respectively. Signals from the β-ester at 1722 cm^{-1} are much stronger than the signals from the α-ester at 1581 cm^{-1},[16] which illustrates the higher reactivity of the β-carboxylic group than the α one (see Scheme 1). It is interesting to note that SAPs with neutralization degrees of 70% and 80% exhibit the highest intensity of carboxylate carbonyl group peaks (connected to sodium ions), even higher than SAPs with a higher neutralization degree (85%). The explanation is that for NDs >80%, most of the monosodium citrate (MSC) is not incorporated into the SAP in view of the relatively low reactivity of MSC. Since SAPs with higher NDs than 85% are completely water-soluble, it is impossible to purify them by rinsing with water. Therefore, the FTIR spectra of these systems are absent in Fig. 4.

As mentioned earlier, besides the molecular structure, the cross-link density is also a key parameter for the absorbing performance and biodegradability (see section 3.6). Fig. 5 clearly shows the following trend: with increasing ND, SAPs have lower G' values at temperatures $\gg T_g$, which indicates a lower cross-link density and accordingly a higher swelling capacity.

3.4. Composition analysis of SAPs

It is well known that neutralization plays an important role in the absorbing power of SAPs. Since MSC has a relatively low reactivity, not all fed MSC monomers can get incorporated into the 3D network structure of SAPs during synthesis and subsequent thermal cross-linking. After the production of SAPs,
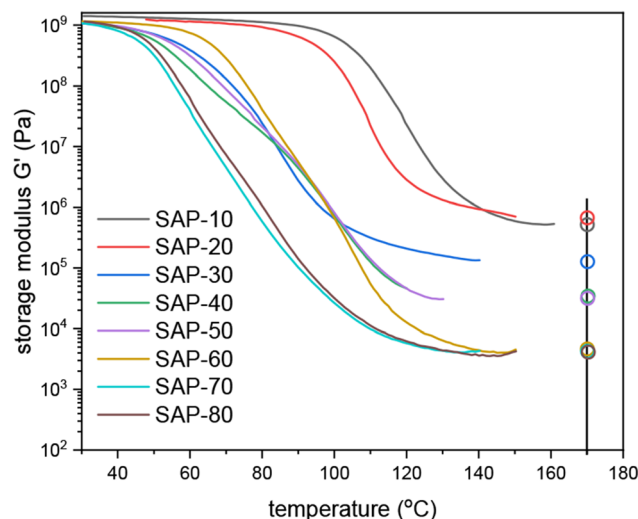
even after the cross-linking treatment in the oven and depending on the ratio of the three monomers in the feed, a larger or smaller part of the SAP particles and unreacted monomers can still be soluble in liquid-like water because of insufficient cross-linking. Usually, part of the unreacted MSC stays in the product after the synthesis of the SAPs, either as an unreacted monomer or incorporated into non-crosslinked water-soluble oligomeric chains, and it can be washed out with water. The content of unreacted MSC can be measured indirectly by elemental analysis (EA) of the Na content of the insoluble part of the SAP compared to the initially present amount of Na. In Fig. 6(a), it can be seen that the Na content of unextracted SAPs is close to the theoretical value calculated from the monomer feed ratio because both reacted and unreacted MSC as well as MSC present in loose oligomeric chains stay in the product. With increasing neutralization degrees, the extracted SAPs prove to have higher Na contents, which is proved by both elemental analysis and EDS (Fig. 6(a) and (b), respectively). There is a difference between the theoretical value (based on the monomer feed ratio) and the value measured for the extracted SAPs, which is in line with the fact that MSC has a lower reactivity with GLY than CA. When the neutralization degree is 30% or lower, the Na contents of the soluble parts of the SAPs are higher than the value calculated for the initial MSC monomer content (10.7 wt%). Such high Na contents in the soluble parts indicate that almost no MSC incorporation into the SAP structure has occurred. The highest Na content in the unextracted and extracted SAPs is achieved when the neutralization degree is 80%, which is in line with the FTIR experiments described above, and this is the composition expected to exhibit the highest water absorption capacity of all studied compositions of this GLY/CA/MSC-based SAP (see further). In
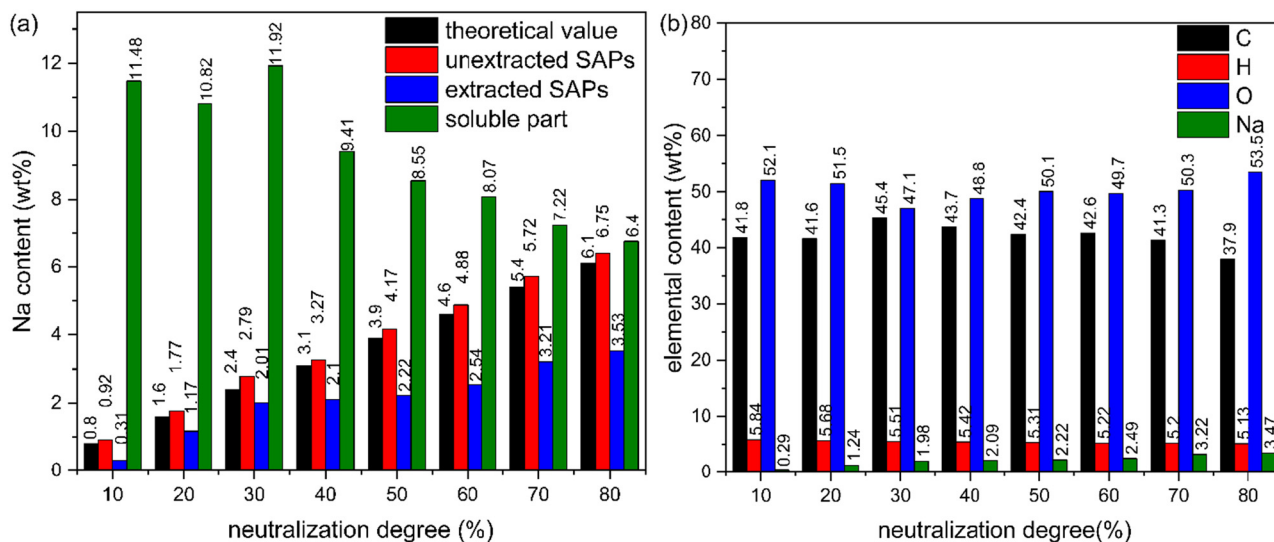
Fig. 6 Plots of composition analysis. (a) Na content of thermally cross-linked (at 140 °C), extracted and unextracted SAPs (ground for 180 s) and of the soluble part determined by elemental analysis. The theoretical value is calculated from the monomer feed ratio. (b) Elemental content (C, H, O, Na) determined by EDS (wt%) of extracted, thermally cross-linked SAPs (cross-linked at 140 °C and ground for 180 s) with different NDs.

Fig. 6(b), it can be observed that the difference between the elemental fractions of C, H and O for different extracted SAPs is negligible, but there is a clear increasing trend of Na content with increasing neutralization degree, resulting in an increasing absorbing capacity as will be shown further in Fig. 7.
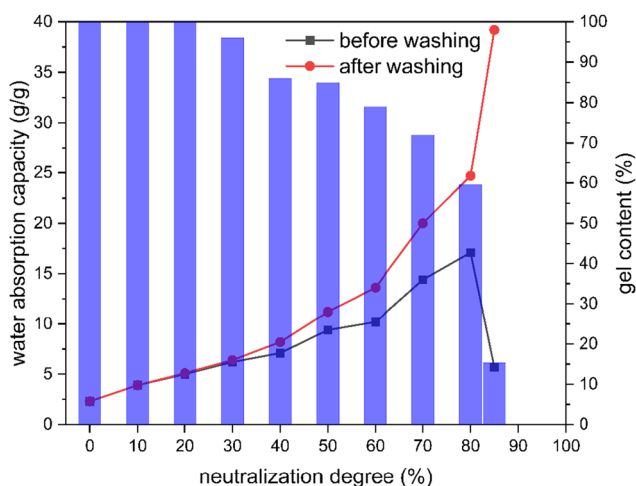

Fig. 7 Plot of water absorbency and gel content of SAPs (cross-linking temperature: 140 °C; grinding time: 180 s) *versus* the neutralization degree or mol% MSC in the mixture of the acidic monomers, before (■) and after washing (●). Blue vertical bars indicate the gel content of the SAPs (cross-linking temperature: 140 °C; grinding time: 180 s) with different NDs. Note: for SAPs with NDs not higher than 30%, the margin of error of water absorption capacity is ± 0.5 g g^{-1}; for SAPs with NDs in the range of 40% to 60% (included), the margin of error of water absorption capacity is ± 1 g g^{-1}; for SAPs with NDs higher than 70% (included), the margin of error of water absorption capacity is ± 2 g g^{-1}; the margin of error of gel content is $\pm 0.5\%$.

3.5. Absorption capacity

As shown in Fig. 7, water absorbencies both before and after washing out (extraction) of the total soluble part of the SAP increase with increasing ND until 80% (from 2.5 ± 0.5 to 18 ± 2 g g^{-1} for the water absorbency before washing and from 2.5 ± 0.5 to 24 ± 2 g g^{-1} for the water absorbency after washing, respectively). These results about gel content are in line with the cross-linking density results mentioned in Fig. 5.

In this work, it has been found that SAPs produced from only CA and GLY, without incorporating MSC, have poor absorbing performance (about 2.5 g g^{-1} in deionized water, DW). In view of this observation, sufficient neutralization is necessary to develop SAPs with excellent absorption capacity. Therefore, in this study a part of the CA was replaced by MSC to introduce sodium ions into our SAPs. As ionic hydrophilic groups, –COONa moieties expand the 3D network of SAPs by electrostatic repulsion and thereby enhance the osmotic pressure difference between the inner and the outer side of the SAPs and accordingly improve the water absorbing performance when these SAPs come into contact with water. With increasing ND, the Na$^+$ content in the SAPs increases (see Fig. 6), which leads to enhanced electrostatic interactions and an enhanced internal osmotic pressure of the cross-linked network. The mentioned expansion of the SAP network structure by electrostatic repulsion between different polymer chains generates more free space, thereby enhancing the accommodation of water. A higher internal osmotic pressure will drive more water entering the SAPs to achieve osmotic pressure equilibrium. However, with the increasing content of MSC in the monomer feed, the amount of non-neutralized carboxylic acid groups will decrease, and thus the chance that OH functionalities from GLY moieties will encounter COOH functionalities from CA moieties and react with ester groups will

Paper

Green Chemistry

decrease, which will result in a lower cross-link density. If this cross-link density becomes too low, even a water-soluble polymer may be formed, totally unsuitable to act as an SAP.

As stated before, unreacted and water-soluble MSC may be left in the system after the SAP synthesis and cross-linking procedure. The water-soluble part of the SAP particles will not contribute to the water absorbing performance. Accordingly, there will be a difference between the absorbing performance of extracted SAPs and unextracted SAPs, since the polymer chains and MSC monomer that are not chemically attached to the SAP network will occupy space where no water can be accommodated and the soluble part of the SAP may only partly be replaced by water molecules. For the evaluation of the absorbance capacity of SAPs, the data obtained for the extracted ones are more relevant. Because of this, the water absorbency after washing is more relevant and can provide more guidance for the production of the most promising SAPs. An increasing ND implies an increasing number of Na^+ ions present in the SAP. However, with a higher amount of less reactive MSC present during synthesis (starting from 30% ND), the content of the unreacted monomer and the water-soluble part will increase as well, which results in a decreasing gel content. When the ND exceeds 80%, *viz.* 90% and 100%, the product is totally water-soluble and useless as an SAP. To find the critical point from which the water absorbency will not increase with further increasing ND, 85% ND was investigated. Interestingly, the non-extracted SAP with an ND of 85% has a much lower water absorbency than SAP-80, most probably related to a too high water-soluble content that limits the entrance and accommodation of water, while its water absorbency after washing is really high (around 40 g g^{-1}). The drawback of this SAP with an ND of 85% is that its gel content is only around 15%, which implies an extremely low SAP yield after the cross-linking procedure. The results presented in Fig. 7 provide useful guidance for the production of CA/GLY-based SAPs: the neutralization degree (MSC content) cannot be higher than 80% in order to obtain SAP products with practical value.

3.6. Biodegradability

One of the main goals of this study is to find out whether the thermally cross-linked SAPs, produced from bio-based monomers by polycondensation, are biodegradable. This biodegradability is crucial for applications in cosmetic products, as soil improvers and in disposed diapers and female care products, to avoid the formation of persistent microplastics in nature. It has been reported that several linear aliphatic polymers possess excellent biodegradability, such as polyhydroxyalkanoates (PHA),[32,33] polybutylene succinate (PBS),[34] polylactic acid (PLA),[35] *etc*. Given that the linear aliphatic SAP precursors of this study are only thermally cross-linked and that most, if not all, cross-linking reactions are based on the esterification between residual –COOH groups originating from CA and residual –OH groups originating from GLY moieties, it was expected that the thermally cross-linked SAPs produced from these SAP precursor polymers would exhibit satisfactory biodegradability. This assumption is based on the possible hydro-

lysis of both the main chain polymer and the ester-based cross-links, keeping in mind that usually the first step initiating biodegradation implies hydrolysis of the polymer material into smaller chain parts that are digestible by the micro-organisms present in the activated sludge.[36–38]

According to the OECD 301F Standard for the biodegradation test of polymer materials, the biodegradability test needs to be performed for a period of at least 28 days. (The detailed method can be found in the ESI.†) In this study, three SAP samples (SAP-20, SAP-70, and SAP-80), either unextracted or extracted, were selected for the biodegradability test, and these SAPs were all characterized for their exact chemical composition (as $C_cH_hO_oNa_{na}$) by elemental analysis and weighed according to the OECD 301F Standard. A well-known biodegradable material, sodium acetate, was chosen as the positive reference in these biodegradability tests. It should be mentioned that even for sodium acetate, the biodegradability cannot reach 100% because a proportion of the carbon and oxygen atoms will be consumed by the bacteria to produce biomass.[39,40] In this study, OECD 301F is chosen as the standard for the test substances. According to the OECD 301F standard, if after 28 days the biodegradability is over 60%, the polymer can be regarded as being readily-biodegradable; the biodegradability test results are presented in Fig. 8. Interestingly, an obvious initiation period can be observed for the extracted samples (Fig. 8(b)), whereas this is not the case for the non-extracted samples. This is probably because there are still unreacted monomers and low molecular weight chains inside the unextracted SAPs and the size of these monomer molecules is small enough to be digested by the bacteria, while for the extracted systems, only cross-linked polymers are present, which cannot move through the cell walls of the micro-organisms. It will take some time for the bacteria to secrete enzymes and break down the polymer chains by hydrolysis to small pieces, which can be assimilated by bacteria.[40] It can be seen in Fig. 8(a) that for the unextracted samples, SAP-80 exhibits biodegradability after 28 days of over 60%, whereas the other two SAPs exhibit lower biodegradability. This is owing to the fact that unextracted SAP-80 has a much lower gel content (less than 60%) than the other two (around 75% for SAP-70 and 100% for SAP-20, Fig. 7), which means that unextracted SAP-80 has a higher content of relatively easily biodegradable unreacted monomers and fewer cross-linked species. For the extracted samples, after 28 days, none of the tested samples exhibit higher biodegradability than 60%, which means that none of these extracted samples are easily biodegradable. Extracted SAP-20 (less MSC used during synthesis) shows really poor biodegradability (less than 2% after 28 days) because it has probably a higher cross-link density as illustrated by a higher G' value at temperature $\gg T_g$ (Fig. 5) and a low polarity which makes it difficult for the water and micro-organism to enter the network. Extracted SAP-70 and SAP-80 show comparable biodegradability, most probably because of rather comparable cross-linking densities, in agreement with Fig. 5, and SAP-70 and SAP-80 have quite comparable MSC moiety contents and polarities. Even though none of
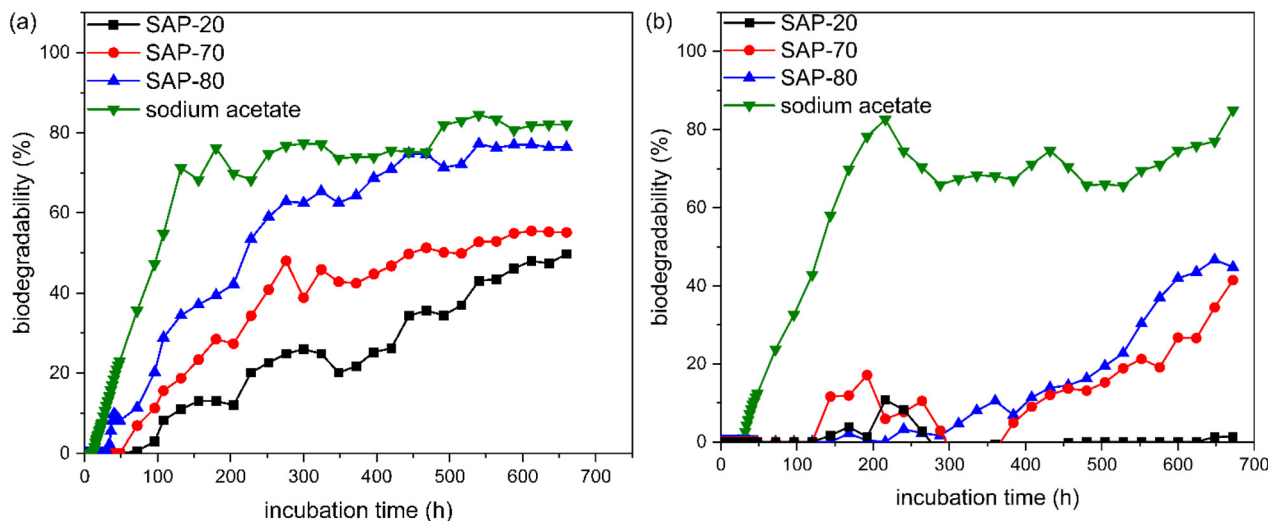
Fig. 8 Biodegradability *versus* incubation time of several SAPs prepared in this study: (a) unextracted samples and (b) extracted samples. Sodium acetate is used as a readily degradable reference material.

the SAPs can be regarded as an easily biodegradable polymer, all tested SAPs show a significant degree of biodegradability after 28 days in the activated sludge. If the incubation time is extended, most likely a much larger part of the SAPs described in this study will be biodegraded, since all connections between the monomeric residues in the main chain polymers as well as the cross-links in the SAPs are of the hydrolyzable ester type. The sterically hindered and partly secondary ester groups in the cross-links will hydrolyze slower than the primary ester groups present in the original SAP precursors. Compared with a benchmark petroleum-based commercial SAP product, the CA-based SAPs show lower water absorption capacity, but much higher biodegradability (details in the ESI†).

4. Conclusion

In summary, SAP precursor polymers were synthesized from CA, MSC, and GLY with different compositions by polycondensation at 130 °C without any catalyst. The number-average and weight-average molecular weights of these SAP precursor polymers were in the range of $0.5–0.7 \times 10^3$ g mol^{-1} and $1.1–17.9 \times 10^3$ g mol^{-1}, respectively. Most of the SAP precursor polymers were water soluble except for PGC, PGC$_{90}$M$_{10}$, and PGC$_{80}$M$_{20}$. These SAP precursor polymers were thermally cross-linked at different temperatures for 1 h to synthesize SAPs. As the cross-linking temperature increases from 140 to 165 °C, the cross-link density increases as well, which was proved by DMTA measurements for SAP-80 as an example. By measuring the absorption capacities of the same SAP cross-linked at different temperatures (ground afterwards), 140 °C was found to be the optimal cross-linking temperature. After extraction of the soluble part and grinding, the resulting SAPs were characterized by particle size analysis, FTIR, elemental analysis, a water absorption property test and a biodegradability test. SAP-80s

with particle sizes of around 65 µm showed the fastest water absorption rate; SAPs with smaller particle sizes than this will encounter gel-blocking effects, which results in fast absorption rates in the beginning but also in much lower maximum absorption capacities; SAP-80s with larger particle sizes exhibit comparable water absorbing capacities but show a slower absorption rate, fully in line with a measured lower BET surface area. With increasing neutralization degree, the SAPs exhibit better water absorbing performance until 80% ND, but at the same time, a higher water-soluble content was observed, implying a lower yield of useful SAP material. Although SAP-85 has even higher water absorbency (close to 40 g g^{-1}), SAP-80 most probably exhibits the most useful combination of a relatively high water absorption capacity $(24 \pm 2$ g g$^{-1})$ and a relatively high gel content after cross-linking of 60%. SAPs with NDs over 85% are water-soluble. In addition, all SAPs show some biodegradability. The biodegradability increases with increasing ND and lower cross-link density. For an ND of 80% (based on the weighed-in CA/MSC monomer ratio), after 28 days, the biodegradability of the SAP is around 40%. Most likely, higher residence times in the activated sludge will further enhance the degree of biodegradation.

These thermally cross-linked, biodegradable SAPs, synthesized from fully bio-based monomers and having high water absorbency, have high potential to be used in application areas like hygienic products (diapers and female care products), cosmetics and agricultural applications like soil conditioners, in all application areas replacing persistent microplastic-generating materials by biodegradable alternatives.

Author contributions

Jingying Chen designed and performed the experiments, analysed the data, and drafted the manuscript. Deelan Yen Chan,

Conflicts of interest

The authors declare that they have no known competing financial interests or personal relationships that could have appeared to influence the work reported in this paper.

Acknowledgements

References

1 F. Masuda and Y. Ueda, Superabsorbent Polymers, in *Encyclopedia of Polymeric Nanomaterials*, ed. S. Kobayashi and K. Müllen, Springer Berlin Heidelberg, Berlin, Heidelberg, 2015, pp. 2351–2366.

2 Y. Bachra, F. Damiri, M. Berrada, J. Tuteja and A. Sand, Introduction of Superabsorbent Polymers, in *Properties and Applications of Superabsorbent Polymers: Smart Applications with Smart Polymers*, ed. S. Arpit and T. Jaya, Springer Nature Singapore, Singapore, 2023, pp. 1–18.

3 J. Chen, J. Wu, P. Raffa, F. Picchioni and C. E. Koning, *Prog. Polym. Sci.*, 2022, **125**, 101475.

4 Super Absorbent Polymers (SAP) Market, https://www.marketsandmarkets.com/Market-Reports/super-absorbent-market-177336849.html.

5 *RAC backs restricting intentional uses of microplastics*, 2020.

6 S. R. D. Petroudy, J. Ranjbar and E. R. Garmaroody, *Carbohydr. Polym.*, 2018, **197**, 565–575.

7 J. Z. Ma, X. L. Li and Y. Bao, *RSC Adv.*, 2015, **5**, 59745–59757.

8 B. X. Cheng, B. Y. Pei, Z. K. Wang and Q. L. Hu, *RSC Adv.*, 2017, 7, 42036–42046.

9 E. L. Krasnopeeva, G. G. Panova and A. V. Yakimansky, *Int. J. Mol. Sci.*, 2022, **23**, 15134.

10 P. A. Mistry, M. N. Konar, S. Latha, U. Chadha, P. Bhardwaj and T. K. Eticha, *Int. J. Polym. Sci.*, 2023, **2023**, 4717905.

11 K. Supare and P. A. Mahanwar, *Polym. Bull.*, 2022, **79**, 5795–5824.

12 D. L. Qiao, H. S. Liu, L. Yu, X. Y. Bao, G. P. Simon, E. Petinakis, *et al.*, *Carbohydr. Polym.*, 2016, **147**, 146–154.

13 X. F. Ma and G. H. Wen, *J. Polym. Res.*, 2020, **27**, 136.

14 M. J. Zohuriaan-Mehr, A. Pourjavadi, H. Salimi and M. Kurdtabar, *Polym. Adv. Technol.*, 2009, **20**, 655–671.

15 M. Klein and E. Poverenov, *J. Sci. Food Agric.*, 2020, **100**, 2337–2340.

16 H. J. Kim, J. M. Koo, S. H. Kim, S. Y. Hwang and S. S. Im, *Polym. Degrad. Stab.*, 2017, **144**, 128–136.

17 Y. Chen, Y. F. Liu and H. M. Tan, *J. Appl. Polym. Sci.*, 2010, **117**, 2233–2240.

18 Y. Liu, Y. F. Zhu, B. Mu, Y. S. Wang, Z. J. Quan and A. Q. Wang, *Polym. Bull.*, 2022, **79**, 935–953.

19 A. H. Alberts and G. Rothenberg, *Faraday Discuss.*, 2017, **202**, 111–120.

20 A. Calmon-Decriaud, V. Bellon-Maurel and F. Silvestre, Standard Methods for Testing the Aerobic Biodegradation of Polymeric Materials. Review and Perspectives, in *Blockcopolymers - Polyelectrolytes – Biodegradation*, ed. V. Bellon-Maurel, A. Calmon-Decriaud, V. Chandrasekhar, N. Hadjichristidis, J. W. Mays, S. Pispas, *et al.*, Springer Berlin Heidelberg, Berlin, Heidelberg, 1998, pp. 207–226.

21 U. Pagga, *Chemosphere*, 1997, **35**, 2953–2972.

22 OECD guideline for testing of chemicals, 1992.

23 P. W. Carrico and B. V. Nathan, *Polyacrylate superabsorbent post-polymerization neutralized with solid, non-hydroxyl neutralizing agent*, WO9852979, 1998, Amcol International Corp.

24 E. Mohammadifar, A. Bodaghi, A. Dadkhahtehrani, A. Nemati Kharat, M. Adeli and R. Haag, *ACS Macro Lett.*, 2017, **6**(1), 35–40.

25 J. Chen, J. Wu, T. Veldhuis, F. Picchioni, P. Raffa and C. E. Koning, *ACS Sustainable Chem. Eng.*, 2025, **13**, 559–570.

26 W. Zou, L. Yu, X. X. Liu, L. Chen, X. Q. Zhang, D. L. Qiao, *et al.*, *Carbohydr. Polym.*, 2012, **87**, 1583–1588.

27 S. Mehra, S. Nisar, S. Chauhan, G. Singh, V. Singh and S. Rattan, *Polym. Chem.*, 2021, **12**, 2404–2420.

28 H. Omidian, S. A. Hashemi, P. G. Sammes and I. Meldrum, *Polymer*, 1999, **40**, 1753–1761.

29 K. M. Lee, J. H. Min, S. Oh, H. Lee and W. G. Koh, *React. Funct. Polym.*, 2020, **157**, 104774.

30 H. Wack and M. Ulbricht, *Ind. Eng. Chem. Res.*, 2007, **46**, 359–364.

31 F. Masuda and Y. Ueda, Superabsorbent Polymers, in *Encyclopedia of Polymeric Nanomaterials*, ed. S. Kobayashi and K. Müllen, Springer Berlin Heidelberg, Berlin, Heidelberg, 2021, pp. 1–18.

32 E. Rudnik, 11 - Biodegradability Testing of Compostable Polymer Materials, in *Handbook of Biopolymers and Biodegradable Plastics*, ed. S. Ebnesajjad, William Andrew Publishing, Boston, 2013, pp. 213–263.

33 K. W. Mereeboer, M. Misra and A. K. Mohanty, *Green Chem.*, 2020, **22**, 5519–5558.

34 M. Barletta, C. Aversa, M. Ayyoob, A. Gisario, K. Hamad, M. Mehrpouya, *et al.*, *Prog. Polym. Sci.*, 2022, **132**, 101579.

35 Y. Tokiwa and B. P. Calabia, *Appl. Microbiol. Biotechnol.*, 2006, **72**, 244–251.

36 V. M. Pathak and Navneet, *Bioresour. Bioprocess*, 2017, **4**, 15.

37 N. Lucas, C. Bienaime, C. Belloy, M. Queneudec, F. Silvestre and J.-E. Nava-Saucedo, *Chemosphere*, 2008, **73**, 429–442.

38 R. Müller, *Biodegradability of Polymers: Regulations and Methods for Testing*, Biopolymers Online, 2005, DOI: **10.1002/3527600035.bpola012**.

39 S. Chinaglia, M. Tosin and F. Degli-Innocenti, *Polym. Degrad. Stab.*, 2018, **147**, 237–244.

40 European Commission: Directorate-General for Environment, M. Hilton, L. Geest Jakobsen, S. Hann and E. Favoino, *et al.*, *Relevance of Biodegradable and Compostable Consumer Plastic Products and Packaging in a Circular Economy*, Publications Office, 2020, **https://data.europa.eu/doi/10.2779/497376**.